forests

MDPI

Article

Ecophysiological Responses of Three Tree Species to a High-Altitude Environment in the Southeastern Tibetan Plateau

Jirui Gong [1,*], Zihe Zhang [1], Chunlai Zhang [1], Jiaqiong Zhang [1] and An Ran [2,*]

[1] State Key Laboratory of Surface Processes and Resource Ecology, College of Resources Science and Technology, Faculty of Geographical Science, Beijing Normal University, Beijing 100875, China; 201621190002@mail.bnu.edu.cn (Z.Z.); clzhang@bnu.edu.cn (C.Z.); jqzhang@nwsuaf.edu.cn (J.Z.)

[2] Department of Veterinary and Biomedical Sciences, University of Minnesota, 1971 Commonwealth Avenue, 205 Veterinary Science, Saint Paul, MN 55108, USA

* Correspondence: jrgong@bnu.edu.cn (J.G.); ran.an@uky.edu (A.R.); Tel./Fax: +86-10-5880-5726 (J.G.)

Received: 17 November 2017; Accepted: 15 January 2018; Published: 23 January 2018

Abstract: This paper measured the ecophysiological responses of *Populus cathayana* Rehd., *Salix longistamina* C. Wang et P. Y. Fu., and *Ulmus pumila* L. to high altitude in the Tibetan Plateau based on changes in water relations, gas exchange, and chlorophyll fluorescence. *P. cathayana* and *U. pumila* have higher survival rates than *S. longistamina*, but the latter has highest biomass. *S. longistamina* has higher water-use efficiency (*WUE*), lower transpiration rates (*E*), higher water potential (Ψ), highest light saturation point (LSP) and higher photosystem II (PSII) photochemistry efficiency (F_v'/F_m') and non-photochemistry quenching (*NPQ*) than the other species, and is thus adapted to its habitat for afforestation. *U. pumila* has lower *E*, light compensation point (*LCP*), dark respiration (R_d), F_v'/F_m' and electron transport rate (*ETR*), with higher Ψ, apparent quantum yield (*AQY*), net photosynthetic rate (P_n) and non-photochemical quenching (*NPQ*), which helps it maintain water balance and utilize weak light to survive at high altitude. Relative low *WUE*, Ψ, R_d, *NPQ*, with high *E*, P_n, F_v'/F_m' and biomass, imply that *P. cathayana* is more suitable for shelterbelt forests than for a semi-arid habitat. These three species can adapt to high-altitude conditions by different physiological mechanisms and morphological characteristics, which can provide a theoretical basis for afforestation and forest management in the Qinghai Tibetan Plateau.

Keywords: high-altitude environment; gas exchange; water relation; chlorophyll fluorescence; water use efficiency

1. Introduction

Climate change affects the distribution, population structure, and growth dynamics of plants [1,2]. Survival of a species in a particular environment requires the ability to adapt to the habitat's characteristics, and, plants have developed a wide range of physiological responses to cope with environmental stresses [3]. Plants either adjust their photosynthetic performance to their environment or adjust their morphological and physiological traits to maintain a homeostatic photosynthetic performance [4,5]. The Tibetan Plateau of western China (also known as the Qinghai-Tibetan Plateau) is the world's largest and highest plateau. Its harsh and complex climatic conditions limit the distribution and diversities of plants due to the effects of high altitude (above 3000 m asl), which include high solar irradiance, reduced CO_2 and O_2, exposure to strong winds, shallow soils, low temperatures, and low availability of water and nutrients [6,7]. Although these characteristics are not favorable for plant growth, many species survive and grow under these conditions by developing special adaptation mechanisms [6]. Understanding how these adaptations affect tree growth is important for researchers interested in predicting the response of forests of the Tibetan Plateau to future climate change.

Three tree species are important parts of the plateau's vegetation. *Populus cathayana* Rehd. is a native Chinese species that is distributed mainly in northern, southwestern, and central China, covering a large geographic range [8,9]. The species has strong resistance to stressful environments and is an important genetic resource, particularly for forest shelterbelts and planting to restore degraded land [10]. *Ulmus pumila* L. is also a native Chinese species, with a long history of cultivation. It develops a deep and widespread root system, and is highly resistant to drought and cold, especially in harsh environments such as that of the Tibetan Plateau [11]. It provides important ecosystem services such as soil and water conservation and the prevention of wind erosion and blowing sand, and also provides high-quality timber; in many of the regions where it grows, it cannot be replaced by other species [12]. *Salix longistamina* C. Wang et P. Y. Fu is mainly distributed in the Tibetan Plateau and the surrounding region, where it mainly grows in valleys and river plains [13]. The species can be used for protection of river banks against erosion, stabilization of sandy soils, and as a windbreak [14]. The species has strong resistance against pests and diseases, and high tolerance of drought and poor soils [15]. Like *U. pumila*, it has a deep and widespread root system [16].

Despite the ecological importance and many favorable characteristics of these species, their ecophysiology and adaptive mechanisms have been poorly studied, particularly at the high altitudes of the Tibetan Plateau. Plant species adapt to adverse environments by different plastic responses, such as physiological or morphological adjustments [17].

Under high illumination levels such as those on the Tibetan Plateau, damage to a plant's photosynthetic apparatus can be severe; this damage can be revealed by a reduction in the variable fluorescence parameter [18]. The photosynthetic efficiency of many plants decreases under stress, which is correlated with a decrease in photochemical quenching of chlorophyll fluorescence and an increase in non-photochemical quenching (*NPQ*) [19,20]. Thus, studies of chlorophyll fluorescence provide insights into a plant's responses to stress. These measurements have the advantage of being non-destructive and rapid, and they also provide information on the utilization and dissipation of light energy [21].

In the present study, our goal was to assess the physiological adaptations of the three local species to the stresses they encounter at high elevation in the southeastern Tibetan Plateau by examining the responses of their morphological characteristics (i.e., survival rate, biomass, height), water relations, gas exchange, and photosynthetic apparatus (i.e., fluorescence properties). Thus, we have proposed two main hypotheses: (1) these three species can adapt to high-altitude conditions using different physiological mechanisms; and (2) *Salix longistamina* is more adapted to harsh conditions with higher *WUE* and photosynthetic activity. The results of this study will contribute to our understanding of the adaptation mechanisms of three species in high altitude and light intensity, low temperature and soil moisture environment. Moreover, the present study could provide some guidance for forest management, cultivation and afforestation in the Tibetan Plateau.

2. Materials and Methods

2.1. Study Site

Our field measurements were carried out in 2010 near Sangye town in the middle reaches of Tibet's Yarlung Zangbo River (29°19′ N, 91°30′ E), at an elevation of approximately 3500 m asl. The area has a cool-temperate semi-arid continental monsoon climate, but with considerable variation within the plateau. The total annual precipitation ranges between 300 and 450 mm. The mean annual temperature ranges between 5 and 9 °C, with maximum temperatures in June and July of 18 to 32 °C and minimum temperatures in February and January of −16 to −37 °C. The frost-free period averages 140 days, and the average total number of sunlight hours reaches 3092 annually.

Seedlings of the three species were from local seed nursery and planted in the spring of 2007 to stabilize an area of sandy soils and improve the ecological environment of a pediment on the northern slopes of the Nyainqentanglha Mountains that are covered with sand sheets, on the northern bank of

the Yarlung Zangbo River. The planting density was about 625 trees per hectare. The species were planted in separate stands with one species of each stand at the same site, separated by at least 10 m to avoid competition between the mature trees (Figure 1). *U. pumila* and *P. cathayana* seedlings were planted with 1m height. The shoots of *S. longistamina* were cut into 15-cm long pieces, each containing three to four buds and soaked in water for 12 h. Then, the cuttings of *S. longistamina* were planted at the site. The study site was located about 20 m above the river, and the local water table was about 8 m below the surface. At the time of our measurements, sunrise occurred at around 08:00 and sunset occurred at around 20:00.

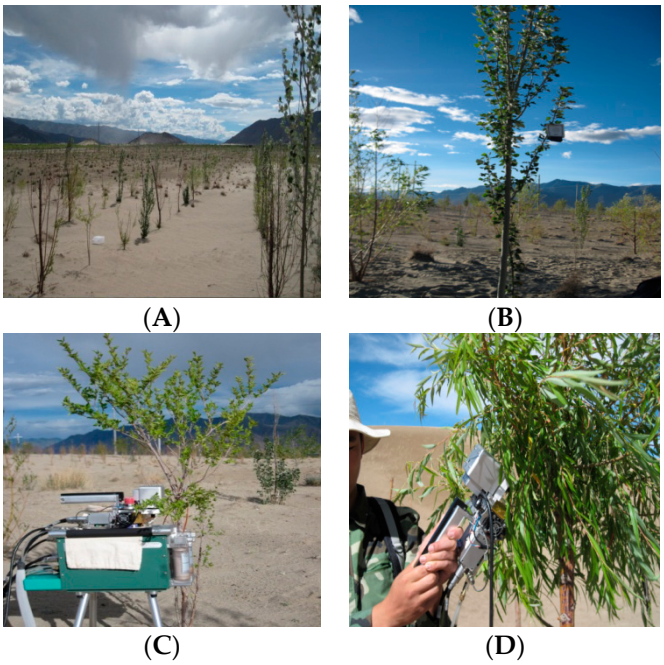

Figure 1. Photos of three species grown in the study site, Yarlung Zangbo River area, Tibet. (**A**) Study site; (**B**) *Populus cathayana*; (**C**) *Ulmus pumila*; (**D**) *Salix longistamina*.

Soil water content was determined from soil samples taken from the center of the root zone (a depth of 60 cm) on the dates of measurement. The samples were dried to constant mass at 105 °C and the mass was expressed as a percentage of the water content. The water content was very low (Table 1). The water content is highest at 0–10 cm depth in all three stands of these tree species.

Table 1. Soil water content of 4 depths in 3 stands at the study site.

Species	Depth (cm)			
	0–10	**10–20**	**20–40**	**40–60**
Populus cathayana	2.78	1.94	2.32	1.38
Ulmus pumila	1.28	0.55	0.79	1.52
Salix longistamina	2.34	2.15	1.23	0.95

2.2. Leaf Gas Exchange

Leaf gas exchange of mature, fully expanded leaves of three individuals of each species was measured on clear, cloudless days (14 and 15 July) in 2010 between 08:00 and 20:00 using an LI-6400 portable photosynthesis system (LI-COR, Lincoln, NE, USA). Each set of three plants came from one of the three stands. Five replications were measured for the current mature foliage on each individual. For these individuals, we measured net photosynthetic rate (P_n), transpiration (E), the intercellular

CO_2 concentration (Ci), stomatal conductance (g_s), the relative humidity (RH), air temperature (T_a), and leaf temperature (T_l). Water use efficiency (WUE) of each species was then obtained by the following equation.

$$WUE = P_n/E \quad (1)$$

2.3. Leaf Water Potential

After the gas-exchange measurements, we measured leaf water potential (Ψ) with a WP4 Dew-point Potential Meter (Decagon Devices, Pullman, WA, USA). We used six fully expanded leaves from the tops of each individual, with three individuals per species. Calibration of the device was checked hourly.

2.4. Photosynthetic Light Response Curves

We obtained photosynthetic light-response curves at 2-h intervals from 9:00 to 11:00 at a range of light intensities (from 0 to 2600 μmol m^{-2} s^{-1}) using a LI-6400-02 Portable Photosynthetic System (LI-COR, Lincoln, NE, USA). The irradiance response was measured at 25 °C and an RH of 50%. CO_2 concentration (400 μmol mol^{-1}) and photosynthetic parameters of each species were obtained after fitting the light response data [22]:

$$A = [A_{max}\ (I - I_c)\ \alpha_c] \ /\ [A_{max} + (I - I_c)\ \alpha_c] \quad (2)$$

where A is net photosynthesis rate, A_{max} the maximal net photosynthesis rate, I_c the light compensation point, I the light intensity, and α_c the quantum efficiency. Dark respiration rate R_d is calculated from the relationship describing the light-limited part of the photosynthesis light response curves:

$$A = \alpha_c I - R_d \quad (3)$$

For $I = I_c$, $A = 0$ and $R_d = \alpha_c I$.

2.5. Diurnal Course of Chlorophyll Fluorescence

Variable chlorophyll a fluorescence was measured with a LI-COR portable LI-6400-40 pulse-amplitude-modulation fluorometer (Li-Cor 6400; Li-Cor, Lincoln, NE, USA). For these measurements, we maintained mature, fully expanded leaves, still attached to the branch, in darkness overnight. Before each measurement, samples were held in darkness for more than 30 min at ambient temperature. We measured maximum fluorescence (F_m) and minimum fluorescence (F_o) simultaneously in the dark. We then exposed the leaves to a photosynthetic photon flux density ($PPFD$) of 1000 μmol photons m^{-2} s^{-1} for more than 3 min to measure the maximum fluorescence (F_m') and steady-state fluorescence (F_s) in the light-adapted state after P_n stabilized. We performed these measurements every 2 h from 08:00 to 20:00 on sunny days.

We calculated the maximum photochemical efficiency of PSII using the formula $(F_m - F_o)/F_m = F_v/F_m$, where F_v represents variable fluorescence. We estimated the effective quantum yield of PSII (ΦPSII) using the equation $\Delta F/F'_m = (F'_m - F_s)/F'_m$ [23]. We calculated photochemical quenching (q_P) as $(F'_m - F_s)/(F'_m - F_o)$ [24], and non-photochemical quenching (NPQ) as $F_m/F_m' - 1$ [25]. We calculated the electron transport rate (ETR) as ΦPSII × PAR × 0.5 × 0.84 [26].

2.6. Survival Rate, Height, Biomass

We examined survival rate, crown and height of three species in the middle of growing season in 2010. At the end of growing season, biomass production and allocation of the three species were measured by means of destructive sampling with three replicates. Then, biomass samples were dried at 75 °C to constant weight.

2.7. Data Analysis

Measurements for each species were compared using analysis of variance (ANOVA). Differences among the species were evaluated using the least significance difference (LSD) method and Tukey test with a significance level of $p < 0.05$, including morphological characteristics (height, biomass, survival rate and crown), water relations (water potential, *WUE*, *E* and *VPD*), gas exchange characteristics (P_n, g_s, C_i), chlorophyll fluorescence parameters (i.e., F_v/F_m, *NPQ*). Data were standardized before the analysis. All statistical analyses were performed using SPSS 18.0 software (SPSS Inc., IBM, Chicago, IL, USA).

3. Results

3.1. Morphological Characteristics

The survival rates (over 3 years), crown, height and biomass among the three species in the study are significantly different ($p < 0.05$). *U. pumila* has the highest survival rate (Table 2, $p < 0.05$). The survival rates of *P. cathayana*, *U. pumila* and *S. longistamina* are 93.80%, 83.83% and 71.70% respectively. The crown diameter of the three species ranges from 45.00 cm × 45.00 cm to 78.00 cm × 63.00 cm ($p < 0.05$). *S. longistamina* has the largest crown and biomass, and *P. cathayana* has the highest height among the three species ($p < 0.05$).

Table 2. Morphological characteristics of the three species grown at the study site.

Species	Survival Rates (%)	Crown Diameter (cm × cm)	Height (cm)	Total Biomass (g)
Populus cathayana	83.83 ± 2.75	45.00 × 45.00	182.33 ± 3.18	381.41 ± 7.08
Ulmus pumila	93.80 ± 5.52	56.00 × 67.00	167.00 ± 5.77	209.61 ± 4.73
Salix longistamina	71.70 ± 3.06	78.00 × 63.00	122.75 ± 1.73	608.97 ± 29.94

3.2. Water Relations

The water potential, transpiration and water use efficiency are significantly different in the species ($p < 0.05$). The diurnal course of water potential shows similar circadian rhythms in all three species with clear diurnal changes (Figure 2A). The Ψ of *P. cathayana* is lower than those of the other species throughout the day (Figure 2A, $p < 0.05$). The *VPD* of the species is not significant. The difference in vapor pressure (*VPD*) follows a similar diurnal pattern in all stands, with the lowest value at sunrise and *VPD* increasing to a maximum at around 14:00 to 16:00 (Figure 2B).

The diurnal changes in *E* of *S. longistamina* and *U. pumila* show two peaks, the first of which appears at about 12:00 and the second appears at about 18:00, whereas *P. cathayana* shows a single peak at about 12:00; *P. cathayana* has the highest *E* and *U. pumila* the lowest (Figure 2C, $p < 0.05$).

The water use efficiency of *S. longistamina* is generally higher than that of other two species, but the diurnal course of *WUE* differs among the three species ($p < 0.05$). In the morning, the *WUE* of *P. cathayana* is lower than that of the other two species, and increases slowly to a maximum at about 14:00 and18:00. *WUE* in the morning follows similar patterns for *S. longistamina* and *U. pumila*, with two peaks at about 10:00 and 14:00 (Figure 2D).

3.3. Gas Exchange

The net photosynthetic rate, stomatal conductance and intercellular carbon dioxide concentration reach a significant level among the species ($p < 0.05$). P_n is highest for *P. cathayana* and lowest for *U. pumila* (Figure 3A, $p < 0.05$). However, the diurnal changes of P_n show a similar pattern with two peaks in all three species. The diurnal trends are similar for g_s, but *U. pumila* and *S. longistamina* differ little in their patterns, with the first peak appearing at 12:00 for *S. longistamina*, which is 2 h earlier than peak P_n for this species. *Populus cathayana* has a higher g_s than the other two species until about

16:00 (Figure 3B,C, $p < 0.05$). The diurnal changes of C_i are decreased first and increased later. The C_i of *S. longistamina* is lowest during the day ($p < 0.05$).

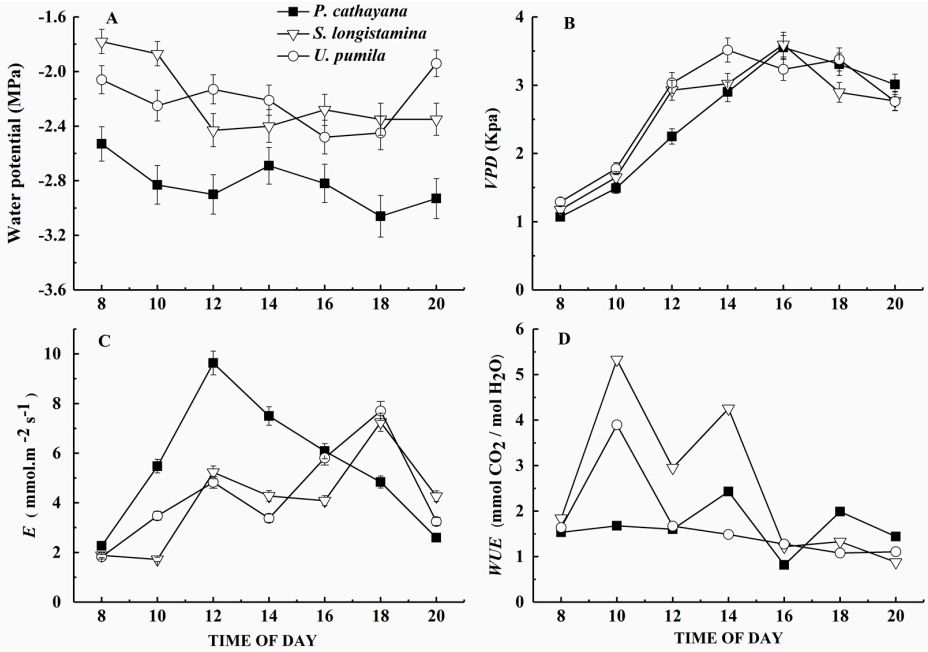

Figure 2. Diurnal course of (**A**) leaf water potential (Ψ), (**B**) vapor-pressure deficit (*VPD*), (**C**) transpiration rate (*E*), and (**D**) water-use efficiency (*WUE*) of *P. cathayana*, *S. longistamina*, and *U. pumila*. Each point represents the mean and standard error of five replicates.

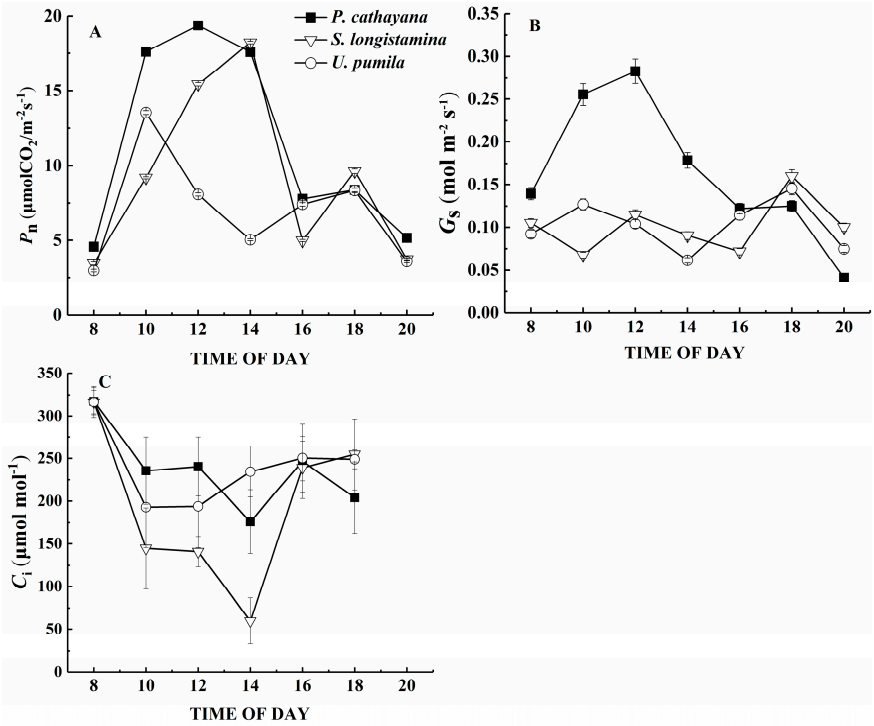

Figure 3. Diurnal course of (**A**) net photosynthetic rate (P_n); (**B**) leaf stomatal conductance (g_s); and (**C**) the internal CO_2 concentration (C_i) in *P. cathayana*, *S. longistamina*, and *U. pumila*. Each point represents the mean and standard error of five replicates.

3.4. P_n-Light Response Curves

The P_n of the three species initially increases with increasing irradiance, and eventually reaches the *LSP* (Figure 4). The curve and P_{max} for *P. cathayana* is obviously higher than those for the other species ($p < 0.05$). The differences of *LSP*, *LCP* and R_d of three species are significant ($p < 0.05$). *S. longistamina* and *P. cathayana* have higher *LSP* and *LCP* than *U. pumila* (Table 3, $p < 0.05$). *S. longistamina* has the higher R_d (3.31 μmol m^{-2} s^{-1}) than other species ($p < 0.05$). *P. cathayana* and *S. longistamina* have the lower *AQY* than *U. pumila* ($p < 0.05$).

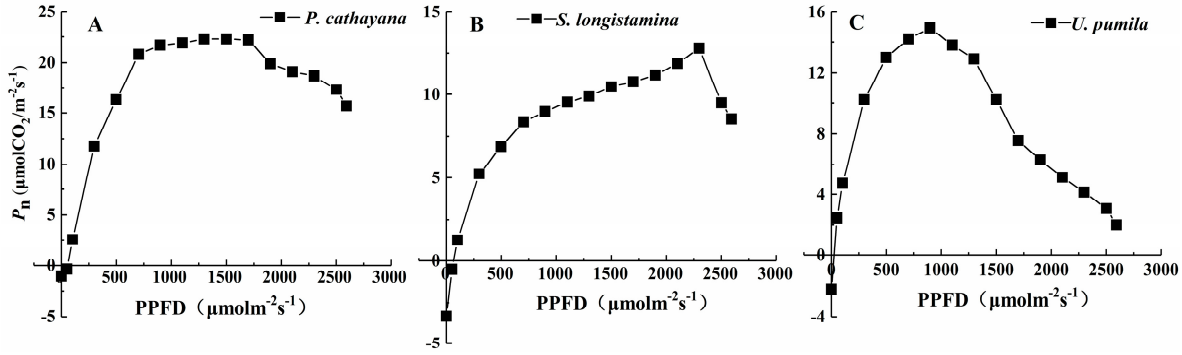

Figure 4. The light saturation curves for net photosynthesis (P_n) as a function of irradiance (*PPFD*) for the leaves of *P. cathayana*, *S. longistamina*, and *U. pumila.* Values represent the means of five replicates.

Table 3. Differences in photosynthetic parameters between *P. cathayana*, *S. longistamina*, and *U. pumila*: maximum photosynthetic rate (P_{max}), light-saturation point (*LSP*), light-compensation point (*LCP*), dark respiration rate (R_d), and apparent quantum yield (*AQY*). Values represent means and standard errors of six replicates.

Species	P_{max} (μmol CO_2 m^{-2} s^{-1})	*LSP* (μmol m^{-2} s^{-1})	*LCP* (μmol m^{-2} s^{-1})	R_d (μmol m^{-2} s^{-1})	*AQY* (μmol CO_2 $μmol^{-1}$)
P. cathayana	22.30 ± 2.14	1791.67 ± 33.29	39.89 ± 3.69	1.02 ± 0.09	0.0448 ± 0.0012
S. longistamina	12.80 ± 3.11	2290.00 ± 28.35	73.01 ± 4.54	3.31 ± 0.15	0.0454 ± 0.0014
U. pumila	14.90 ± 2.32	998.33 ± 13.58	26.35 ± 2.25	2.23 ± 0.12	0.0686 ± 0.0011

3.5. Chlorophyll Fluorescence Parameters

We observed distinct patterns in the diurnal course of the potential quantum yield of PSII (i.e., F_v/F_m) (Figure 5A). F_v/F_m in *P. cathayana* and *U. pumila* isn't significantly different, but both show a mid-day depression. *U. pumila* shows an especially strong reduction in F_v/F_m during the day, reaching a minimum of 0.59 at around 18:00; thereafter, it increases slowly and recovers to near its value at the start of the day. However, F_v/F_m in *S. longistamina* decreases throughout the day, with neither a mid-day depression nor full recovery at sunset. Of the three species, *S. longistamina* has the highest F_v/F_m during most of the day ($p < 0.05$).

F_v'/F_m' in *S. longistamina* and *U. pumila* shows similar diurnal changes (Figure 5B). Among the three species, F_v'/F_m' is highest in *S. longistamina* and lowest in *U. pumila* ($p < 0.05$).

In response to the rapid increase in *PPFD*, ΦPSII decreases sharply after sunrise (Figure 5C). ΦPSII in *S. longistamina* and *U. pumila* increases rapidly later in the day, reaching values similar to the pre-dawn values by sunset. ΦPSII of *P. cathayana* does not show full recovery by sunset. ΦPSII is generally higher in *S. longistamina* and *P. cathayana* than in *U. pumila* ($p < 0.05$).

The diurnal course of *ETR* shows different patterns for the three species (Figure 5D). *ETR* of *U. pumila* initially increases to a peak at 10:00, then decreases until about 12:00 and subsequently recovers. *ETR* of *P. cathayana* and *S. longistamina* has similar patterns, but the maximum value reaches at 14:00 and 16:00, respectively. *ETR* is significantly higher in *S. longistamina* and *P. cathayana* than in *U. pumila* ($p < 0.05$).

In all three species, $1 - q_p$ is significantly different, and increases sharply after sunrise, reaching a maximum value by around 10:00, then decreases slowly (Figure 5E, $p < 0.05$). At 16:00 and 18:00, respectively, $1 - q_p$ reaches the second, lower peak in *P. cathayana* and *S. longistamina*; thereafter, it decreases again. *S. longistamina* has lowest $1 - q_p$ during a day ($p < 0.05$).

After sunrise, the *NPQ* of all three species increases (Figure 5F), and the diurnal changes show two peaks and a mid-day depression. *NPQ* of *S. longistamina* is significantly higher than other species at 12:00 ($p < 0.05$).

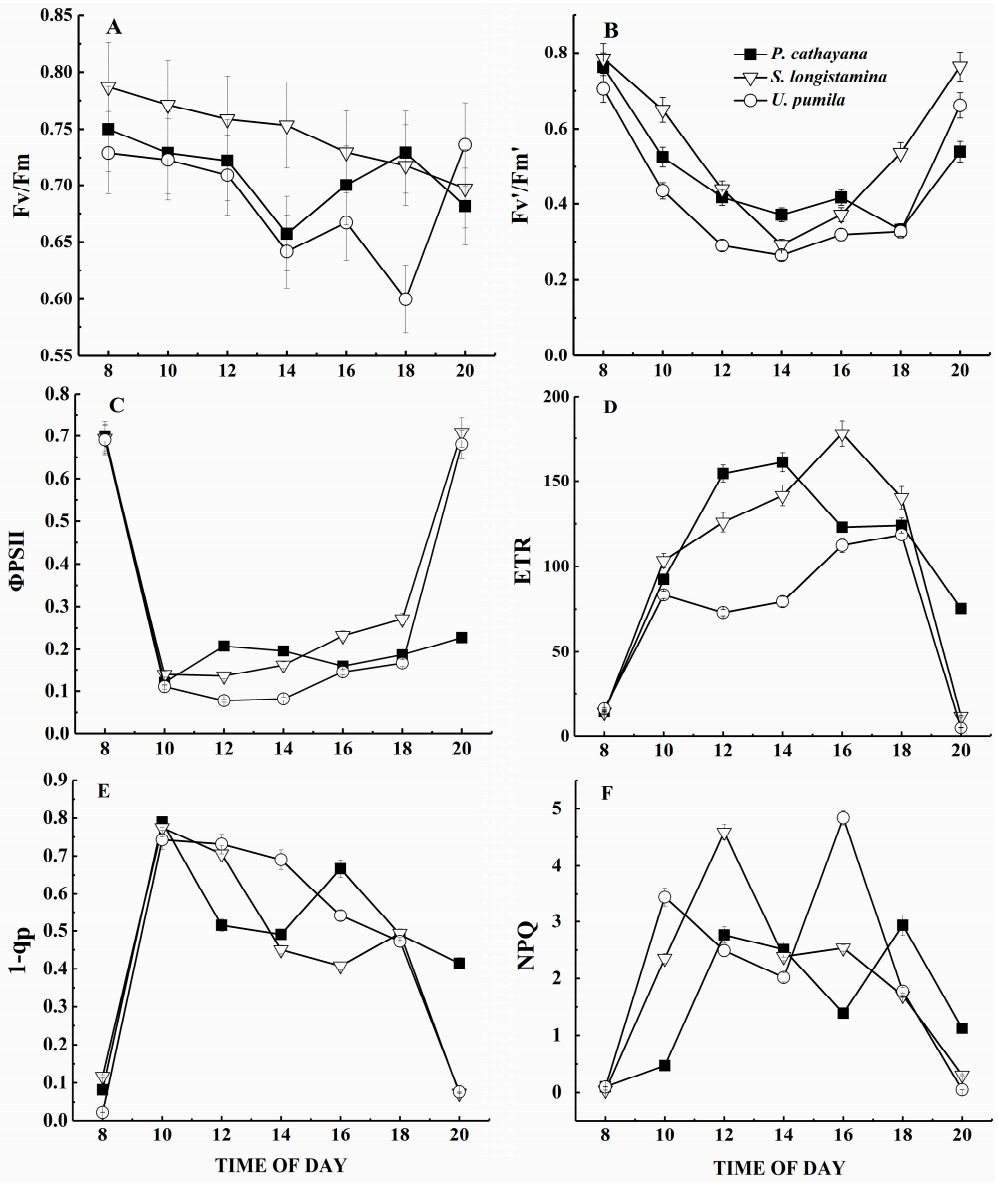

Figure 5. Diurnal course of (**A**) potential quantum efficiency of photosystem II (F_v/F_m); (**B**) the maximum efficiency of photosystem II (F_v'/F_m'); (**C**) the quantum yield of photosystem II (ΦPSII); (**D**) the electron transport rate (*ETR*); (**E**) the degree of closure of the PSII reaction centers ($1 - q_p$); and (**F**) non-photochemical quenching (*NPQ*). Values represent means and standard errors of five replicates.

4. Discussion

4.1. Morphological Characteristics

The survival rate of plants is influenced by many biotic and abiotic factors such as pests, water shortage, and high irradiance [27]. A high survival rate of plants suggests high adaptation ability [28]. The survival rates of *P. cathayana*, *U. pumila* and *S. longistamina* in the study are 93.80%, 83.83% and 71.70%, indicating these species have strong adaption ability in the Qinghai-Tibet Plateau [29]. *S. longistamina* has highest biomass and crown among the species, suggesting a strong tolerance to resource-limited conditions [30]. The reason probably is the strong root system and high P_n and *WUE* of *S. longistamina*. The root system of *Salix* is sensitive to external stress such as salinity [31]. *S. longistamina* may increase its root-to-shoot ratio in high irradiance conditions, which helps it absorb water and nutrients for accumulating larger biomass [32].

4.2. Water Relations

Water is one of the fundamental factors for plants influencing their growing process. However, in many regions like the Qinghai-Tibetan Plateau, water resources are becoming seriously limited. Thus, plants will utilize water sources more efficiently by changing their water regimes [33]. Ψ reflects a plant's water status, and determines the plant's ability to maintain its water balance by absorbing water from the soil and from neighboring cells. The higher Ψ of *S. longistamina* and *U. pumila* suggests that they sustain better water relations under water-limited conditions than *P. cathayana*, probably as a result of their massive root system, which can exploit deep soil moisture [34,35]. The root system of *Salix* has strong root anchorage, which helps roots embed in soils, and *Ulmus* can generate new roots rapidly and thus increase root surface area [36]. These characteristics indicate the strong water absorption capacity of these three species.

WUE is the ratio of P_n and E, which is an important physiological parameter that can help to explain a plant's ability to maintain water equilibrium [37]. Increased *WUE* has been proved an adaptation to semi-arid and arid environment [38]. The higher *WUE* in *S. longistamina* indicates that it conserves water better than the other species. Its low E and high P_n support this conclusion [39]. *S. longistamina* and *U. pumila* have higher Ψ and *WUE* with lower E, which suggests their better water relations under water-limited conditions, and their suitability for afforestation in the Qinghai Tibetan Plateau [40]. Adversely, *WUE* of *P. cathayana* is lower because of its higher P_n and E. The higher g_s of *P. cathayana* may result in higher E. It opens stomata to assimilate carbohydrates rapidly at first then closes to avoid water loss. This diurnal trend indicates that *P. cathayana* is sensitive to changes in the external environment and can utilize resources optimally [41]. The higher P_n of *P. cathayana*, combined with its low *WUE* and high $-E$ and a large leaf area, make this species more suitable for use in a forest shelterbelt where water is abundant for the purpose of preventing erosion and decreasing wind speed to protect crops and soils [42]. These physiological adaptions help the species to survive in the semi-arid, high-altitude area.

4.3. Gas Exchange

Plant survival in a given environment depends on the plant's ability to adapt to the habitat, moreover, plants can develop different ecophysiological characteristics even in similar habitats [43]. In the present study, three species show different gas-exchange characteristics. The higher P_n of *P. cathayana* and *S. longistamina* indicates that they have higher photosynthetic capacity than *U. pumila* under the conditions [44]. However, P_n of all three species remains greater than 0 μmol CO_2 m^{-2} s^{-1} throughout the day during this part of the growing season, suggesting that they are capable of adapting to a high-irradiance environment. The diurnal changes in P_n show a similar pattern with two peaks in all three species. A similar phenomenon was reported for other high-altitude plants [44]. Farquhar and Sharkey [45] suggested that a reduction in photosynthetic capacity is caused by stomatal closure, as well as by non-stomatal factors. When g_s and C_i decrease simultaneously, the decline in P_n is caused

mainly by stomatal closure. During the mid-day depression in P_n for *P. cathayana* and *S. longistamina*, both g_s and C_i decrease, so stomatal limitation of photosynthesis may explain the mid-day depression in these species. The temperature at noon reaches its peak so that these two species close stomata to avoid water loss and reduce CO_2 absorption [46]. In contrast, the mid-day depression of P_n for *U. pumila* occurs when C_i changes in the opposite direction to g_s, suggesting that the mid-day depression is primarily attributable to non-stomatal factors. High light intensity resulted in non-stomatal limitation, as well as lower Rubisco activity, electron transport rates, carboxylation efficiency and damage to PSII reaction center, which is also influenced by some biochemical indexes (e.g., plant hormone) [47]. Plants growing in the field are susceptible to photoinhibition under environmental stress [48]. Photoinhibiton decreases the photosynthetic efficiency under stress, in which input of photons exceeds demand [49]. In the present study, F_v/F_m, F_v'/F_m', and ΦPSII of all three species decrease with increasing *PPFD* and then recovered in the afternoon as *PPFD* decreases, suggesting that photoinhibition occurs in all three species and may be another cause for the depression in P_n [50]. We will discuss this in more detail in the section *Photosynthetic efficiency*.

4.4. Photosynthesis Curve

P_{max} has been widely used to compare the ecophysiological characteristics of plants [51]. P_n of the three species increases with increasing irradiance, and reaches the *LSP* in all three species. Consequently, they are likely to be able to protect their photosynthetic apparatus against photo-degradation [52]. *P. cathayana* has higher P_{max} and *LSP* and lower *LCP* and R_d, suggesting its better light use ability. *P. cathayana* can grow fast in high altitude conditions with higher P_n and biomass. The largest *LSP* of *S. longistamina* indicates that it has higher light-use efficiency in the study area, and largest biomass and *WUE* of *S. longistamina* suggests a better adaptation to the high irradiance [53]. *LCP* reflects the ability of plants to make use of low irradiance [28]. The higher the value of *AQY*, the more efficiently photosynthesis converts light energy and the higher the photosynthetic capacity [54]. *U. pumila* cannot make full use of the available *PPFD* for much of the day. However, the lower *LCP* and R_d of *U. pumila* with highest *AQY* suggests that the species can tolerate shade and utilize weak light better than the other species, thereby increasing the accumulation of photosynthate [55]. These are the main reasons why *U. pumila* can survive on the Tibetan Plateau despite obvious photoinhibition and low biomass compared with the other species. Therefore, the three species have different photosynthesis mechanisms to utilize light to form more carbon assimilate to survive under high-altitude conditions.

4.5. Photochemistry Efficiency

Photoinhibition has been observed in many plants growing naturally in the field, and is revealed by a mid-day decrease in F_v/F_m [56]. In our study, there are clear differences in F_v/F_m among the three species. F_v/F_m of *P. cathayana* and *U. pumila* decreases to a lower level than that of *S. longistamina* at mid-day, but recovers almost completely at sunset, suggesting that photoinhibition in these species is a photoprotective mechanism accomplished through thermal dissipation of excess energy, as suggested by the mid-day increase of *NPQ* in both species [57]. Photoinhibition can be caused by photodamage not only to the photosynthetic apparatus but also to photoprotective mechanisms through thermal dissipation of excess energy [58]. In our study, F_v/F_m remains lower than 0.80 throughout the day, indicating that all three species are stressed by the high irradiance. This suggests the presence of chronic photoinhibition and damage to PSII's reaction centers, resulting in photodamage during the summer at the high altitude of the study area [59]. Thus, we hypothesize that photoinhibition in all three species resulted both from a photoprotective process and from photodamage.

The maximum PSII efficiency (F_v'/F_m') can be thought of as the efficiency with which PSII's antennae absorb photons and deliver them to open PSII reaction centers [60]. F_v'/F_m' is higher for *S. longistamina* and *P. cathayana* than for *U. pumila*, and shows a proportionally smaller decrease during the day than occurs for *U. pumila*. This suggests that *U. pumila* has less capacity to utilize the high

excitation energy that is available through photosynthetic electron transport. This is supported by the lower *ETR* for *U. pumila* [61].

The actual PSII efficiency can be used to estimate the rate of photochemical reactions in terms of the absorbed light that is utilized in photochemistry [23]. ΦPSII and *ETR* are both high in *S. longistamina* and *P. cathayana* and low in *U. pumila*, indicating a high degree of phenotypic plasticity of the photosynthetic apparatus in these species [62]. Our study supports previous results, in which the operating efficiency is often linearly related to P_n [23]. The decrease in actual PSII efficiency under excess light can be caused by two processes: an increase in closure of PSII reaction centers and a decrease in the efficiency of excitation capture in PSII through photoprotective thermal dissipation of excess excitation energy before it reaches the PSII reaction centers [63]. With higher photosynthetic efficiency and with lower *NPQ* and a lower degree of closure of the PSII reaction centers, *P. cathayana* exhibits less thermal dissipation and closure of the PSII reaction centers than the other species, combined with high *LSP* and *LCP* and lowest R_d, which means that it captures more excitation energy to drive photosynthetic electron transport and larger biomass [64]. In contrast, *S. longistamina* has higher *NPQ* and a lower degree of closure of the PSII reaction centers than in *P. cathayana*. This suggests that the higher biomass in *P. cathayana* and *S. longistamina* results, at least in part, from higher photochemical efficiency [65]. In contrast, *U. pumila* has higher *NPQ* and a higher degree of closure of the PSII reaction centers, in addition to lower *ETR* and *LCP*, implying a higher degree of thermal dissipation [66]. These results suggest that all three species can compensate for high irradiance by changing their utilization of absorbed light through changes in electron transport, but to different extents [67]. The decrease of PSII efficiency in the three species under high irradiance results from a decrease in the efficiency of excitation capture in PSII and by an increase in the degree of closure of the PSII reaction centers [68].

5. Conclusions

Our study suggests that *P. cathayana*, *S. longistamina* and *U. pumila* acclimate efficiently to field conditions in the semi-arid, high-altitude study area. Of the three, *S. longistamina* has the highest *WUE*, *LSP*, biomass, photochemistry efficiency and lowest water loss; therefore, this species is drought-tolerant and capable of surviving well in semi-arid habitats. Despite its lower *WUE*, *U. pumila* has lower *E* and comparable higher water potential, *AQY* and lowest *LCP*, which lets it maintain its water balance and utilize weak light to survive at high altitude. These two species can be used in afforestation for a series of ecosystem services such as soil and water conservation. In contrast, because of low *WUE*, *LCP* and R_d and highest P_n and *E*, *P. cathayana* is more suitable for sites with abundant water like forest shelterbelts than for a desert habitat. These three species all can tolerant high-altitude conditions via different physiological mechanisms and morphological characteristics. Above all, *S. longistamina* can utilize resources optimally in the Tibetan Plateau. Our results can provide understanding of physiological mechanisms about these species' survival in this area. In future forest management in the region, *S. longistamina* can be considered as an economically important species for cultivation to prevent soil erosion and improve the harsh environment.

Acknowledgments: We thank Y.G. Liu, Beijing Normal University, for his field assistance. This study was supported by the National Basic Research Program of China (Grant No. 2013CB956001) and by the National Natural Science Foundation of China (Grant No. 40771069).

Author Contributions: Jirui Gong and Chunlai Zhang conceived and designed the experiments; An Ran and Jiaqiong Zhang performed the field and laboratory experiments; Jirui Gong analyzed the data; Jirui Gong and Zihe Zhang wrote the paper.

Conflicts of Interest: The authors declare no conflict of interest.

References

1. Devi, N.; Agedorn, F.; Moiseev, P.; Bugmann, H.; Shiyatov, S.; Mazepa, V.; Rigling, A. Expanding forests and changing growth forms of Siberian larch at the Polar Urals tree line during the 20th century. *Glob. Chang. Biol.* **2008**, *14*, 1581–1591. [CrossRef]
2. Qian, C.; Yin, H.; Shi, Y.; Zhao, J.; Yin, C.; Luo, W. Population dynamics of *Agriophyllum squarrosum*, a pioneer annual plant endemic to mobile sand dunes, in response to global climate change. *Sci. Rep.* **2016**, *6*, 1–12. [CrossRef] [PubMed]
3. Okunlola, G.O.; Olusanya, A.O. Physiological response of the three most cultivated pepper species (*capsicum* spp.) in Africa to drought stress imposed at three stages of growth and development. *Sci. Hortic.* **2017**, *224*, 198–205. [CrossRef]
4. Liang, E.Y.; Wang, Y.F.; Xu, Y. Growth variation in *Abies georgei* var. *smithii* along altitudinal gradients in the Sygera Mountains, Southeastern Tibetan Plateau. *Trees* **2010**, *24*, 363–373. [CrossRef]
5. Najafabadi, M.Y.; Ehsanzadeh, P. Photosynthetic and antioxidative upregulation in drought-stressed sesame (*Sesamum indicum* L.) subjected to foliar-applied salicylic acid. *Photosynthetica* **2017**, *4*, 611–622. [CrossRef]
6. Wonsick, M.M.; Pinker, R.T. The radiative environment of the Tibetan plateau. *Int. J. Clim.* **2014**, *34*, 2153–2162. [CrossRef]
7. Roupioz, L.; Jia, L.; Nerry, F.; Menenti, M. Estimation of daily solar radiation budget at kilometer resolution over the Tibetan plateau by integrating Modis data products and a DEM. *Remote Sens.* **2016**, *8*, 504. [CrossRef]
8. Chen, C.; Peng, Y.H. AFLP analysis of genetic diversity in *Populus cathayana* Rehd. originating from Southeastern Qinghai–Tibetan Plateau of China. *Pak. J. Bot.* **2010**, *42*, 117–127.
9. Song, Y.; Ma, K.; Ci, D.; Zhang, Z.; Zhang, D. Biochemical, physiological and gene expression analysis reveals sex-specific differences in *Populus tomentosa* floral development. *Physiol. Plant.* **2013**, *150*, 18–31. [CrossRef] [PubMed]
10. Wu, N.; Li, Z.; Wu, F.; Tang, M. Comparative photochemistry activity and antioxidant responses in male and female *Populus cathayana* cuttings inoculated with arbuscular mycorrhizal fungi under salt. *Sci. Rep.* **2016**, *6*, 37663. [CrossRef] [PubMed]
11. Su, H.; Li, Y.; Liu, W.; Xu, H.; Sun, O.J. Changes in water use with growth in *Ulmus pumila*, in semiarid sandy land of northern China. *Trees* **2014**, *28*, 41–52. [CrossRef]
12. Park, G.; Lee, D.; Kim, K.; Batkhuu, N.O.; Tsogtbaatar, J.; Zhu, J.J.; Jin, Y.; Park, P.S.; Hyun, O.; Kim, H.S. Morphological characteristics and water-use efficiency of siberian elm trees (*Ulmus pumila* L.) within arid regions of northeast Asia. *Forests* **2016**, *7*, 280. [CrossRef]
13. Guillermo, N.; Doffo, S.E.; Monteoliva, M.E.; Rodríguez, V.M.; Luquez, C. Physiological responses to alternative flooding and drought stress episodes in two willow (*Salix* spp.) clones. *Can. J. For. Res.* **2016**, *47*, 174–182. [CrossRef]
14. Karrenberg, S.; Edwards, P.J.; Kollmann, J. The life history of Salicaceae living in the active zone of floodplains. *Freshw. Biol.* **2002**, *47*, 733–748. [CrossRef]
15. Pusz, W.; Urbaniak, J. Foliar diseases of willows (*Salix* spp.) in selected locations of the *Karkonosze mts*. (the giant mts). *Eur. J. Plant Pathol.* **2017**, *148*, 45–51. [CrossRef]
16. Yang, H.; Chu, J.; Lu, Q.; Gao, T. Relationships of native trees with grasses in a temperate, semi-arid sandy ecosystem of northern China. *Appl. Veg. Sci.* **2014**, *17*, 338–345. [CrossRef]
17. Zhang, S.; Zhang, L.; Zhou, K.; Li, Y.; Zhao, Z. Changes in protein profile of *Platycladus orientalis*, (L.) roots and leaves in response to drought stress. *Tree Genet. Genomes* **2017**, *13*, 76. [CrossRef]
18. Robakowski, P.; Laitat, E. Effects of an enhanced ultraviolet–B irradiation on photosynthetic apparatus of several forests coniferous tree species from different locations. *Acta Physiol. Plant.* **1999**, *21*, 283–296. [CrossRef]
19. Lukaszek, M.; Poskuta, J. Chlorophyll a fluorescence kinetics and CO_2 exchange rates in light and in darkness in leaves of tall fescue as affected by UV radiation. *Acta Physiol. Plant.* **1996**, *18*, 345–350.
20. Liu, X.; Wang, Z.; Bao, W.; Li, X.M. Photosynthetic responses of two pleurocarpous mosses to low-level nitrogen addition: A study in an old-growth fir forest. *J. Bryol.* **2015**, *37*, 15–22. [CrossRef]
21. Bilger, W.G.; Schreiber, U.; Bock, M. Determination of the quantum efficiency of photosystem II and of non–photochemical quenching of chlorophyll fluorescence in the field. *Oecologia* **1995**, *102*, 425–432. [CrossRef] [PubMed]

22. Drake, B.G.; Read, M. Carbon dioxide assimilation, photosynthetic efficiency, and respiration of a Chesapeake Bay salt marsh. *J. Ecol.* **1981**, *69*, 405–423. [CrossRef]
23. Genty, B.; Briantais, J.M.; Baker, N.R. The relationship between the quantum yield of photosynthetic electron transport and quenching of chlorophyll fluorescence. *Biochim. Biophys. Acta* **1989**, *990*, 87–92. [CrossRef]
24. Van Kooten, O.; Snel, J.F.H. The use of fluorescence nomenclature in plant stress physiology. *Photosynth. Res.* **1990**, *25*, 147–150. [CrossRef] [PubMed]
25. Bilger, W.; Björkman, O. Role of the xanthophylls cycle in photoprotection elucidated by measurements of light–induced absorbance changes, fluorescence and photosynthesis in *Hedera canariensis*. *Photosynth. Res.* **1990**, *25*, 173–185. [CrossRef] [PubMed]
26. Demmig, B.; Björkman, O. Comparison of the effects of excessive light on chlorophyll fluorescence (77K) and photon yield of O_2 evolution in leaves of higher plants. *Planta* **1987**, *171*, 171–184. [CrossRef] [PubMed]
27. Ceulemans, R.; Deraedt, W. Production physiology and growth potential of poplars under short-rotation forestry culture. *For. Ecol. Manag.* **1999**, *121*, 9–23. [CrossRef]
28. Gong, J.R.; Zhang, X.S.; Huang, Y.M. Comparison of the performance of several hybrid poplar clones and their potential suitability for use in northern China. *Biomass Bioenergy* **2011**, *35*, 2755–2764. [CrossRef]
29. Kaczmarek, D.J.; Coyle, D.R.; Coleman, M.D. Survival and growth of a range of Populus clones in central South Carolina USA through age ten: Do early assessments reflect longer-term survival and growth trends. *Biomass Bioenergy* **2013**, *49*, 260–272. [CrossRef]
30. Major, J.E.; Mosseler, A.; Malcolm, J.W.; Heartz, S. Salinity tolerance of three Salix, species: Survival, biomass yield and allocation, and biochemical efficiencies. *Biomass Bioenergy* **2017**, *105*, 10–22. [CrossRef]
31. Dong, Y.; Yan, M.A.; Wang, H.; Zhang, J.; Zhang, G.; Yang, M.S. Assessment of tolerance of willows to saline soils through electrical impedance measurements. *For. Ecosyst.* **2013**, *15*, 32–40.
32. Mamashita, T.; Larocque, G.R.; Desrochers, A.; Beaulieu, J.; Thomas, B.R.; Mosseler, A.; Major, J.; Sidders, D. Short-term growth and morphological responses to nitrogen availability and plant density in hybrid poplars and willows. *Biomass Bioenergy* **2015**, *81*, 88–97. [CrossRef]
33. Galmés, J.; Flexas, J.; Savé, R.; Medrano, H. Water relations and stomatal characteristics of Mediterranean plants with different growth forms and leaf habits: Responses to water stress and recovery. *Plant Soil* **2007**, *290*, 139–155. [CrossRef]
34. Chen, G.C.; Liu, Z.; Zhang, J.; Owens, G. Phytoaccumulation of copper in willow seedlings under different hydrological regimes. *Ecol. Eng.* **2012**, *44*, 285–289. [CrossRef]
35. Cao, Y.; Ma, C.; Chen, G.; Zhang, J.; Xing, B. Physiological and biochemical responses of *Salix integrathunb*. under copper stress as affected by soil flooding. *Environ. Pollut.* **2017**, *225*, 644–653. [CrossRef] [PubMed]
36. Tanaka, N.; Samarakoon, M.B.; Yagisawa, J. Effects of root architecture, physical tree characteristics, and soil shear strength on maximum resistive bending moment for overturning *Salix babylonica*, and *Juglans ailanthifolia*. *Landsc. Ecol. Eng.* **2012**, *8*, 69–79. [CrossRef]
37. Davies, W.J.; Wilkinson, S.; Loveys, B. Stomatal control by chemical signalling and the exploitation of this mechanism to increase water use efficiency in agriculture. *New Phytol.* **2002**, *153*, 449–460. [CrossRef]
38. Maud, V.; Smith, H.K.; David, C.; Jennifer, D.; Harriet, T.; Marijke, S.; Bastien, C.; Taylor, G. Adaptive mechanisms and genomic plasticity for drought tolerance identified in European black poplar (*Populus nigral.*). *Tree Physiol.* **2016**, *36*, 909–928.
39. Wikberg, J.; Ogren, E. Variation in drought resistance, drought acclimation and water conservation in four willow cultivars used for biomass production. *Tree Physiol.* **2007**, *27*, 1339–1346. [CrossRef] [PubMed]
40. Podlaski, S.; Pietkiewicz, S.; Chołuj, D.; Horaczek, T.; Wiśniewski, G.; Gozdowski, D.; Kalaji, H.M. The relationship between the soil water storage and water-use efficiency of seven energy crops. *Photosynthetica* **2017**, *55*, 210–218. [CrossRef]
41. Landhaüsser, S.M.; Stadt, K.J.; Lieffers, V.J. Photosynthetic strategies of summer green and evergreen understory herbs of the boreal mixed wood forest. *Oecologia* **1997**, *112*, 173–178. [CrossRef] [PubMed]
42. Dhillon, G.S.; Van Rees, K.C.J. Soil organic carbon sequestration by shelterbelt agroforestry systems in Saskatchewan. *Can. J. Soil Sci.* **2017**, *97*, 394–409. [CrossRef]
43. Kattge, J.; Knorr, W.; Raddatz, T.; Wirth, C. Quantifying photosynthetic capacity and its relationship to leaf nitrogen content for global-scale terrestrial biosphere models. *Glob. Chang. Biol.* **2009**, *15*, 976–991. [CrossRef]
44. Weih, M.; Bonosi, L.; Ghelardini, L. Optimizing nitrogen economy under drought: Increased leaf nitrogen is an acclimation to water stress in willow (*Salix* spp.). *Ann. Bot.* **2011**, *108*, 1347–1353. [CrossRef] [PubMed]

45. Farquhar, G.D.; Sharkey, T.D. Stomatal conductance and photosynthesis. *Annu. Rev. Plant Physiol.* **1982**, *33*, 317–345. [CrossRef]
46. Feng, D.; Wang, Y.; Lu, T.; Zhang, Z.; Han, X. Proteomics analysis reveals a dynamic diurnal pattern of photosynthesis-related pathways in maize leaves. *PLoS ONE* **2017**, *12*. [CrossRef] [PubMed]
47. Jiao, L.; Wang, L.; Zhou, Q.; Huang, X. Stomatal and non-stomatal factors regulated the photosynthesis of soybean seedlings in the present of exogenous bisphenol A. *Ecotoxicol. Environ. Saf.* **2017**, *145*, 150–160. [CrossRef] [PubMed]
48. Adams, W.W., III; Diaz, M.; Winter, K. Diurnal changes in photochemical efficiency, the reduction state of *Q. radiationless* energy dissipation, and non-photochemical fluorescence quenching in cacti exposed to natural sunlight in northern Venezuela. *Oecologia* **1989**, *80*, 553–561. [CrossRef] [PubMed]
49. Lu, T.; Meng, Z.; Zhang, G.; Qi, M.; Sun, Z.; Liu, Y.; Li, T. Sub-high temperature and high light intensity induced irreversible inhibition on photosynthesis system of tomato plant (*Solanum lycopersicum* L.). *Front. Plant Sci.* **2017**, *8*, 182. [CrossRef] [PubMed]
50. Li, L.; Pan, X.L.; Hong, L. Responses of photosystem II (PSII) function in leaves and samaras of *Ulmus pumila* to chilling and freezing temperatures and subsequent recovery. *Int. J. Agric. Biol.* **2012**, *14*, 739–744.
51. Kaipiainen, E.L. Parameters of photosynthesis light curve in *Salix dasyclados* and their changes during the growth season. *Russ. J. Plant Physiol.* **2009**, *56*, 445–453. [CrossRef]
52. Ögren, E.; Sjöström, M. Estimation of the effect of photoinhibition on the carbon gain in leaves of a willow canopy. *Planta* **1990**, *181*, 560–567. [CrossRef] [PubMed]
53. Li, J.Y.; Zhao, C.Y.; Li, J.; Yan, Y.Y.; Yu, B.; Han, M. Growth and leaf gas exchange in *Populus euphratica* across soil water and salinity gradients. *Photosynthetica* **2013**, *51*, 321–329. [CrossRef]
54. Cai, Z.Q. Shade delayed flowering and decreased photosynthesis, growth and yield of Sacha Inchi (*Plukenetia volubilis*) plants. *Ind. Crop. Prod.* **2011**, *34*, 1235–1237. [CrossRef]
55. Ďurkovič, J.; Čaňová, I.; Priwitzer, T.; Biroščíková, M.; Kapraľ, P.; Saniga, M. Field assessment of photosynthetic characteristics in Micropropagated and grafted Wych elm (*Ulmus glabra*, huds.) trees. *Plant Cell Tiss. Organ Cult.* **2010**, *101*, 221–228. [CrossRef]
56. Gong, J.R.; Zhao, A.F.; Huang, Y.M.; Zhang, X.S.; Zhang, C.L. Water relations, gas exchange, photochemical efficiency, and Peroxidative stress of four plant species in the Heihe drainage basin of Northern China. *Photosynthetica* **2006**, *44*, 355–364. [CrossRef]
57. Xue, W.; Li, X. Moderate shade environment facilitates establishment of desert phreatophytic species *Alhagi sparsifolia*, seedlings by enlarge fine root biomass. *Acta Physiol. Plant* **2017**, *39*, 7. [CrossRef]
58. Liu, M.Z.; Jiang, G.M.; Li, Y.G.; Niu, S.L.; Cui, H.X. Gas exchange, photochemical efficiency, and leaf water potential in three *Salix* species. *Photosynthetica* **2003**, *1*, 393–398. [CrossRef]
59. Contin, D.R.; Soriani, H.H.; Hernández, I.; Furriel, R.P.M.; Munné-Bosch, S.; Martinez, C.A. Antioxidant and photoprotective defenses in response to gradual water stress under low and high irradiance in two *Malvaceae* tree species used for tropical forest restoration. *Trees* **2014**, *28*, 1705–1722. [CrossRef]
60. Liu, J.; Last, R.L. A chloroplast thylakoid lumen protein is required for proper photosynthetic acclimation of plants under fluctuating light environments. *Proc. Natl. Acad. Sci. USA* **2017**, *114*, 8110–8117. [CrossRef] [PubMed]
61. Tian, Y.; Ungerer, P.; Zhang, H.; Ruban, A.V. Direct impact of the sustained decline in the photosystem ii efficiency upon plant productivity at different developmental stages. *J. Plant Physiol.* **2017**, *212*, 45–53. [CrossRef] [PubMed]
62. Han, Y.; Wang, L.; Zhang, X.; Korpelainen, H.; Li, C. Sexual differences in photosynthetic activity, ultrastructure and phytoremediation potential of *Populus cathayana* exposed to lead and drought. *Tree Physiol.* **2013**, *33*, 1043–1060. [CrossRef] [PubMed]
63. Demmig–Adams, B.; Adams, W.W., III; Logan, B.A.; Verhoeven, A.S. Xanthophyll cycle dependent energy dissipation and flexible PSII efficiency in plants acclimated to light stress. *Aust. J. Plant Physiol.* **1995**, *22*, 249–261.
64. Ding, L.; Wang, K.J.; Jiang, G.M.; Li, Y.G.; Jiang, C.D.; Liu, M.Z.; Niu, S.L.; Peng, Y. Diurnal variation of gas exchange, chlorophyll fluorescence, and xanthophyll cycle components of maize hybrids released in different years. *Photosynthetica* **2006**, *44*, 26–31. [CrossRef]

65. Pierangelini, M.; Ryšánek, D.; Lang, I.; Adlassnig, W.; Holzinger, A. Terrestrial adaptation of green algae *Klebsormidium* and *Zygnema* (charophyta) involves diversity in photosynthetic traits but not in CO_2 acquisition. *Planta* **2017**, *246*, 971–986. [CrossRef] [PubMed]
66. Ruban, A.V. Quantifying the efficiency of photoprotection. *Phil. Trans. R. Soc. B* **2017**, *372*, 1730. [CrossRef] [PubMed]
67. Randriamanana, T.R.; Nissinen, K.; Moilanen, J.; Nybakken, L.; Julkunen-Tiitto, R. Long-term UV-B and temperature enhancements suggest that females of *Salix myrsinifolia*, plants are more tolerant to UV-B than males. *Environ. Exp. Bot.* **2014**, *109*, 296–305. [CrossRef]
68. Dias, M.C.; Pinto, G.; Guerra, C.; Jesus, C.; Amaral, J.; Santos, C. Effect of irradiance during acclimatization on content of proline and phytohormones in micropropagated *Ulmus minor*. *Biol. Plant.* **2013**, *57*, 769–772. [CrossRef]